Engineered Science
DOI: https://dx.doi.org/10.30919/es1252

Vertical Handover-Based Hybrid Radio Frequency/Visible Light Communication Scheme for e-Health Applications

Nivine Guler*

Abstract

Maximizing spectral efficiency and capacity in conventional radio frequency (RF) systems is crucial for indoor wireless communication with high data rate demands. Utilizing visible light communication (VLC) bands addresses this challenge, though VLC's reliance on the line of sight (LoS) connectivity poses obstacles. This paper introduces a vertical handover-based hybrid RF/VLC for intra-software-defined wireless body area network (SDWBAN) architecture to meet diverse quality of service (QoS) requirements. Prioritizing emergency data enhances network reliability. The proposed hard switching algorithm addresses a multi-objective optimization problem, minimizing outage and blocking probabilities, worst-case latency, and packet error rate while maximizing throughput and system fairness. Pareto-simulated annealing efficiently selects either the VLC or RF link to meet system constraints. Simulation results show that the proposed hybrid RF/VLC scheme significantly improves performance, especially at lower signal-to-interference plus noise ratios, with reduced outage probability (25 % to 55 %), enhanced throughput (40 % to 60 %), decreased packet error rate (39 % to 50 %), and improved system fairness (8 % to 10 %) compared to standalone VLC systems.

Keywords: Visible light communication (VLC); Radio frequency (RF); Link selection; Hybrid RF/VLC system; Signal to interference and noise ratio (SINR).
Received: 31 March 2024; Revised: 15 July 2024; Accepted: 17 July 2024.
Article type: Research article.

1. Introduction

Radio frequency (RF) has been the dominant approach to providing wireless connectivity for centuries. However, various challenges incorporate such technology, such as spectrum congestion, interference, security, privacy and safety issues, and energy efficiency. To overcome the above-stated challenges, recently, visible light communication (VLC) technology has emerged to transmit information wirelessly by exploiting the lighting infrastructure of solid-state light sources (*e.g.*, white light-emitting diodes) to provide light-based wireless connectivity.[1] VLC is a relatively new wireless communication technology that makes use of the visible light infrastructure to create light-based wireless communication links. Recently, VLC has become a hot topic in wireless communication networks, causing many researchers to deeply analyze and develop VLC-based schemes to overcome challenges faced by RF networks. VLC technology has been implemented for various wireless network types, such as for indoor, outdoor, vehicular and underwater scenarios. The principal advantages of VLC are the large and unregulated available bandwidth, the inherent security and privacy of optical systems, and the appropriate use in both interference-sensitive environments and radio-free exposure use cases. VLC systems have been used in various medical environments and have been studied by several authors. Recently, hybrid RF/VLC networks have been proposed aiming at exploiting the benefits of both technologies,[1,2] especially in the recent era, where universal lockdown is witnessed due to the coronavirus disease (COVID-19), and everything went online, including the health activities. Such a hybrid RF/VLC network is particularly attractive for sensitive environments such as hospitals, as the combined radio-optical network can be flexibly configured to adapt to scenarios and fulfill their associated requirements.[2] Hybrid RF/VLC technology is very important as it combines the advantages of both RF and VLC standalone systems. Therefore, it adds diversity, increases coverage and decreases power consumption and interference.

Department of Computer Science, University of Central Asia, Naryn, 722918, Kyrgyzstan
**Email:* nivine.guler@ucentralasia.org (N. Guler)

VLC is a new wireless communication technology that exploits the presence of lighting infrastructure to provide light-based wireless links. In recent years, VLC technology has attracted many researchers to implement it in different scenarios, aiming at overcoming the limitations caused by RF technologies. Various networks have been studied using VLC technology, especially in indoor, outdoor, vehicular and underwater scenarios. The main advantages of VLC technology are the large and unregulated available bandwidth,[3] the inherent security and privacy of optical systems,[4] and its safety due to the zero-radio emission. Hence, as an alternative to communication systems that operate in the RF band (3 kHz to 300 GHz), the use of visible light bands (400 THz to 800 THz) for wireless communications has been proposed. Bell and Tainter, in 1880, were the first to present the idea of using light to transmit a signal (photo-phone), as discussed in Ref. [5]. However, transmitting data using a light source was first introduced using a fluorescent lamp.[6] Then, the idea of using fast-switching light-emitting diodes (LEDs) was presented in Ref. [7]. The white LED was used for both illumination and communication in early 2000 by researchers at Keio University.[8] Following this achievement, various studies focused on the use of white LEDs in communication systems. In 2011, the first IEEE standard related to VLC, IEEE 802.15.7, was published by the IEEE 802.15 working group for wireless personal area networks.[3] Fig. 1 illustrates both the strengths and weaknesses of the RF and VLC technologies. As can be seen, high health safety, high security, high spectrum availability, low electromagnetic interference, and low power consumption are more likely offered by VLC bands. RF band supports high mobility and coverage, which can be immune to noise from light resources and penetrate obstacles. Based on the above-mentioned characteristics, several studies investigate how RF and VLC systems can be hybridized in a common system. Therefore, hybrid RF/VLC schemes were proposed to overcome the limitations of both RF and VLC technologies. Shao and Khreishah focused on aggregated and non-aggregated heterogeneous RF/VLC wireless networks where the average system delay is derived for both scenarios.[9] It was clear that the average system delay for aggregated scenarios is lower as compared to non-aggregated scenarios. The outage performance for a hybrid RF/VLC system was studied in the work of Pan *et al.*,[10] considering the light energy harvesting over the downlink. The hybrid system, which consists of a radio and optical orthogonal frequency-division multiplexing (HRO-OFDM) scheme, was proposed in Ref. [11] and combines the different features of RF and VLC links. Kashef *et al.*[12] investigate the energy efficiency of hybrid RF/VLC networks and study the impact of system parameters on energy efficiency. In this paper, we propose a hybrid RF/VLC scheme for intra-software-defined wireless body area network (intra-SDWBAN) for static patients, *i.e.*, mobility of the patient is not considered in this study. The presented study leverages the benefits of both RF and VLC technologies to maintain the network quality of service (QoS). The hybrid implementation of RF and VLC technologies is desired, especially for wireless body area networks (WBANs), where critical or emergency data should be transmitted with the least or no delays. In our presented scheme, we give high priority to sensors sending emergency data. We include the outage probability for the communication bands and the blocking probability of the VLC band in the link selection algorithm. The blocking probability of the VLC band occurs in the intersection of the coverage area of more than one VLC access point (AP). Therefore, in the area where the blocking occurs, an RF band should be selected for communication to ensure the functionality of the system. The switching or hard handover between RF and VLC systems is managed by the software-defined networking (SDN) controller, which oversees the network. The controller assigns a time threshold to prevent the ping-pong effect of unnecessary switching between the two technologies. Hence, the controller tries to keep the communication scenario in the VLC band as much as possible since it provides high data rates with much fewer delays required for sending the emergency data precisely.

The rest of the paper is arranged as follows. Section II describes the related work in literature. Section III describes the proposed hybrid RF/VLC scheme. Section IV presents performance evaluation and analysis. Finally, Section V concludes the paper.

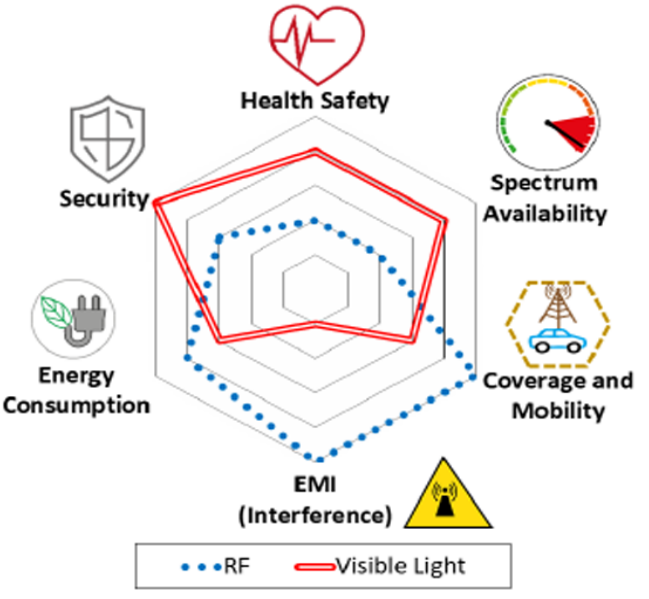

Fig. 1 Advantages and disadvantages of RF and VLC standalone.

2. Related work

The integration of RF and VLC technologies motivated many researchers. Basnayaka and Haas studied the hybrid RF/VLC system, where trade-offs between power and spectrum were investigated.[13] Dynamic load balancing is studied for a hybrid LiFi/WiFi network in Ref. [14] that serves quasi-static users. The movement of users is tiny by LiFi photocells and moving users by WiFi access points. Wang *et al*.[15] and Liang *et al*.[16] proposed a vertical handover scheme for heterogeneous RF/VLC systems.

Haddad *et al*.[17] studied the channel modeling for WBANs, taking into consideration the mobility model of the patients. For different mobility scenarios, they investigated the channel direct current (DC) gain, delay spread, and coherence time. Le *et al*.[18] investigated the shadow impact of indoor mobile VLC on system performance where the channel is considered mobile, with different data rates. Siddiqi *et al*.[19] considered a VLC system with direct current biased orthogonal frequency division multiplexing (DC-OFDM) where resource allocation was done based on the user satisfaction index using simulated annealing to maximize the average user satisfaction index. Simulations show that their method outperforms other well-known heuristic algorithms. Cahyadi *et al*.[20] demonstrated a VLC system using three biosensors that can transmit data via VLC uplink. Different Predefined headers were added to the sent data to differentiate sensors' signals at the receiver end. Minor interference has been reported in the received signal caused by the flux of the ceiling. On the contrary, interference was obviously recorded when multiple sensors sent their data at the same time over an RF link. As a result, VLC presents an alternative solution for transmitting bio signals where these are less susceptible to interference. Dhatchayeny *et al*.[21] presented a VLC-based study to validate the fact that data loss is almost negligible when data is transmitted over VLC rather than over RF. They used electroencephalography (EEG) to monitor data for this study, as EEG signals consist of multiple frequencies related to different parts of the brain; thus, transmitting each frequency separately is critical for proper diagnosis. The reported results showed zero interference in transmission. Ding *et al*.[22] addressed the benefits behind using the combined concepts of VLC and PLC as a backbone in network communication of hospitals; a concept of combining VLC and power line communications (PLC) in hospitals for numerous purposes has been presented.

In the literature, specifically for Hybrid RF/VLC WBAN, two important arguments are mentioned. The first one is that very few have efficiently considered the outage probability and the handover dwell/threshold time concurrently in the link selection process. The handover dwell/threshold time prevents the ping-pong effects caused by frequent switching between RF and VLC bands. The ping-pong effects degrade the overall network performance. Therefore, in our study, we took into account the outage and blocking probabilities concurrently with the handover time threshold in the link selection algorithm to optimally select the communication band. The second argument is that most researchers restrict their system from using the VLC band at the beginning of the simulation. Then, the switching technique is executed by each sensor to decide on which band to use for communication. Such approaches lead to a noticeable number of handovers, which degrade the network performance, especially when blocking probability exists and/or increases. Therefore, in our presented scheme, the system uses the RF band at the beginning of the simulation due to different blocking probabilities. This causes fewer handovers and less degradation of network performance. Besides, to the best of the author's knowledge, there is no reported work on hybrid RF/VLC intra-SDWBAN that considers the blocking and outage probabilities, achieves QoS by prioritizing the emergency data, and maximizes the system fairness at the same time.

The main contributions of this paper are as follows:

- Proposing a vertical handover technique for hybrid RF/VLC-based intra-WBANs to optimally select the communication link by applying the Pareto Simulating Annealing algorithm (PSA) for solving the multi-objective optimization problem;
- Defining the cost function that minimizes the outage and blocking probabilities, worst-case latency, and packet error rate maximizes the system throughput and maximizes the system fairness by taking into consideration the handover time threshold to prevent unnecessary handovers;
- Analyzing the performance of the proposed scheme for different blocking probabilities and comparing it with state-of-the-art schemes;
- Evaluating the performance of the proposed hybrid RF/VLC scheme in comparison with the standalone VLC scheme for different signal-to-interference plus noise ratios;
- Leveraging the concept of SDN by integrating an SDN controller in the hybrid RF/VLC network.

3. Network architecture

In this section, we present the network architecture of the vertical handover-based hybrid RF/VLC system for e-health applications, which includes the system model and the channel model.

3.1 System model

The presented model is similar to the proposed system model by Gupta *et al*.[23] However, here, we considered a hybrid RF/VLC intra-software-defined wireless body area network as shown in scenario (a) of Fig. 2. The model consists of a room of (5×5×3) m^3 with three patients (P), each equipped with low-power body sensors and an SDN controller. The sensors monitor and send the patient's condition to the controller, which is assumed to be placed at the patient's waist. We assume a star network topology that fulfills the requirement defined by IEEE 802.15.7, where all sensors send data to the

SDN controller, which in turn sends the data to a gateway. We also assume an out-of-band SDN architecture where the control messages between sensors and controllers are sent on dedicated paths. The patients are equipped with an RF antenna and photodiode. We employ a hybrid RF/VLC downlink transmission system based on hard switching between VLC and RF channels. We assume one RF AP and four VLC hotspots are mounted on the ceiling of the room, each with an array of 60×60 LEDs as transmitters and also for illumination. The location of VLC transmitters is indicated in Table 1, and the location of sensor nodes is indicated in Table 2. The Lambertian optical source model is used in the VLC transmitter, where the brightness is the same regardless of the patient's angle of view. Therefore, the projection of a VLC hotspot on the ground can be regarded as a circle, as shown in Fig. 2a. The VLC receiver is assumed to be in front of the patient and at a 1.2 m distance from the floor. The SDN controller manages the network, assigns network resources to body sensors, and executes the PSA algorithm to efficiently select the RF link or VLC link for the body sensors. The VLC transmitters utilize the same light wave bandwidth; hence, there is high co-channel interference in the overlapped area of VLC hotspots.[3] Therefore, the VLC link is assumed to be blocked in these areas. An example of the blocking scenario is shown in Fig. 2, where the middle patient is in the coverage area of more than one VLC AP. The coverage area of VLC AP is shown in blue, which is smaller than that of RF, which covers the whole room. The SDN controller plays a vital role in attaining the network QoS by serving the priority-based sensors without causing unnecessary delays. Also, it manages and distributes the network resources among sensor nodes. Based on channel conditions, the controller decides whether to do hard switching between the communication channels. When the controller detects there is a need for handover, it executes the link selection algorithm and calculates the handover delay. The decision to select the communication band is triggered by a time interval, which is called dwell time or handover time threshold, in order to prevent unnecessary handovers that degrade the quality of communication needed for achieving the WBAN's QoS.[4,24] Since choosing the optimal VLC channel among the presented channels is an NP-hard problem, the controller executes the Pareto simulated annealing (PSA).[24] We have formulated our fitness function based on several performance metrics to be used by PSA to choose the optimal VLC link. Fig. 2(b) illustrates the LoS of the VLC channel. Each VLC spot is constituted of 3600 LEDs where radiation patterns are modeled by a Lambertian one with an order m=1 that corresponds to a half-power angle of 60°.

Table 1. VLC transceiver characteristics.

Transmitters	Coordinates [x y z] (m)	T1: [1.25 1.25 3] T2: [1.25 3.75 3] T3: [3.75 3.75 3] T4: [3.75 1.25 3]
Receiver	Half angle of power	60°
	Avg. transmitted power per LED (P_{LED})	10 mW
	Responsivity	0.28 A/W
	Field of view (FOV)	65°

Table 2. Nodes' location.

Node #	Description	Location		Priority
		x-axis	y-axis	
1	EEG	1.52	2.97	√
2	ECG	1.55	1.57	√
3	Glucose	1.55	1.21	√
4	Motion	1.28	1.65	-
5	EMG	1.26	2.18	-
6	Blood Pressure	1.57	1.47	√
7	Pulse OXIMETER	1.6	1.21	-
8	Lactic acid	1.42	2.11	-
9	Accelerometer	1.65	1.65	-
10	Respiratory	1.35	1.7	√
11	Pressure	1.35	1.65	√
12	SDN-controller	1.2	1.2	-

3.2 Channel model

In the proposed model, we assume the receiver is oriented towards the ceiling, where θ=0o. As a result, the VLC channel is mainly characterized by LoS optical paths. The number of VLC APs, sensors, sub-channels per VLC AP, and sub-channels per RF AP is denoted by N, K, nVLC, and nRF, respectively. The set of VLC APs and sensors are denoted as $\mathcal{N} = \{1,\ldots, N\}$ and $\mathcal{K} = \{1,\ldots, K\}$, respectively. Let $\eta VLC = \{1,\ldots,nVLC\}$ and $\eta RF = \{1,\ldots., nRF\}$ represent the sub-channel sets per VLC AP and RF AP, respectively. We assume orthogonal frequency division multiple access (OFDMA) is used for channel modulation where different sensor nodes achieve simultaneous access.

3.2.1 RF channel model

In our proposed scheme, we assume the medical room is equipped with one RF AP of Nakagami-m.[25] In the RF network, the channel gain of an RF sub-channel n is typically as in Eq. (1).[14]

$$h_{k,n}^{RF} = 10^{-PL_k[dB]/10}, \forall n \in \eta RF, \forall k \in \mathcal{K} \quad (1)$$

where $PL_k[dB]$ is the RF path loss of the k-th sensor in dB, which is expressed in Eq.(2).[14]

$$PL_k[dB] = A\, log_{10}(d_k^{RF}) + B + C\, log_{10}(f_c/5) \quad (2)$$

where f_c denotes the carrier frequency in GHz. A, B and C are constants depending on the propagation model. d_k^{RF} represents the Euclidean distance between RF AP and k-th

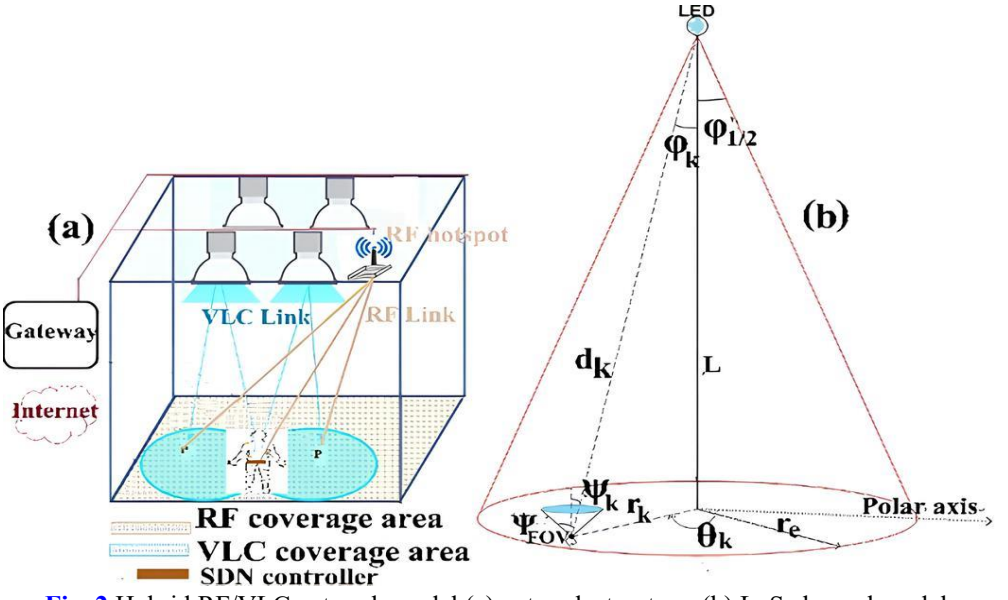

Fig. 2 Hybrid RF/VLC network model (a) network structure, (b) LoS channel model.

sensor. For our model, where LoS is considered, A=18.7, B= 46.8 and C = 20.[26]

For the RF link, we assume the Nakagami-m fading model where the received Signal to interference and noise ratio (SINR) at sensor k of RF sub-channel n has the probability density function (PDF) expressed by Eq. (3).[14,25]

$$f_{\Gamma_{RF}}\left(SINR_{k,n}^{RF}\right)=\left(\frac{m}{\overline{SINR}_{k,n}^{RF}}\right)^{m}\frac{{SINR_{k,n}^{RF}}^{m-1}}{\Gamma(m)}e^{\left(\frac{-SINR_{k,n}^{RF}}{\overline{SINR}_{k,n}^{RF}}\right)m} \quad (3)$$

where m denotes the fading factor and $\overline{SINR}_{k,n}^{RF}$ represents the average SINR of the RF link. The PDF of Gamma distribution can be expressed by Meijer-G function as in Eq. (4).[27]

$$f_{\Gamma_{RF}}\left(SINR_{k,n}^{RF}\right)=\frac{1}{\Gamma(m)\overline{SINR}_{k,n}^{RF}}\mathcal{G}_{0,1}^{1,0}\left[\left(\frac{SINR_{k,n}^{RF}}{\overline{SINR}_{k,n}^{RF}}\right)m\middle|_{m}^{-1}\right] \quad (4)$$

where $\mathcal{G}(.)$ is the Meijer-G function.

3.2.2 VLC channel model

In Fig. 2, we consider a downlink transmission model. The VLC transmitter is located on the ceiling at height L from the kth sensor located at a polar angle from reference axis θt and radius rt on the polar coordinate plane. The maximum radius covered by the LED cell is denoted by re. The PD at each user is assumed to be oriented vertically upwards, and its FOV is denoted by ΨFOV. The angle of incidence and angle of irradiance are denoted by ψt and φt, respectively. Usually, a complete VLC channel consists of both the LoS link and the diffuse components caused by light reflections from interior surfaces in a typical indoor environment. The strongest diffuse component is at least 7 dB (electrical) lower than the weakest LoS component.[4] Therefore, only the LoS link is considered in this work. For indoor VLC, the channel gain of LoS is modeled by the Lambertian emission, where m is the order of the Lambertian model. Therefore, LED follows a Lambertian radiation pattern whose order is given by Eq. (5).

$$\mathrm{m}={}^{-1}/_{log_2\left(cos(\varphi_{1/2})\right)} \quad (5)$$

where $\varphi_{1/2}$ represents the semi-angle of LED at half power.

In the case of having LoS, the Euclidean distance between the LED and the k-th sensor is denoted by dk. It is observed that the DC channel gain, denoted by hk, of the VLC channel between LED and kth sensor is given by Eq. (6).

$$\mathrm{hk}=\frac{A(m+1)\gamma}{2\pi {d_k}^2}cos^{m}(\varphi\mathrm{k})\mathrm{O}(\psi\mathrm{k})\mathrm{g}(\psi\mathrm{k})\cos(\psi\mathrm{k}) \quad (6)$$

where A denotes the PD detection area; $\mathfrak{r}$ represents the responsivity of the PD; O(ψt) represents the gain of the optical filter used at the receiver, and g(ψt) shown in Eq. (7) represents the gain of the optical concentrator.[28]

$$g(\psi_k)=\begin{cases}\frac{\mathfrak{r}^2}{sin^2(\Psi FOV)}, & 0\le\psi_k\le\Psi FOV\\ 0, & \psi_k>\Psi FOV\end{cases} \quad (7)$$

where $\mathfrak{r}$ denotes the refractive index of the concentrator.

Looking at Fig. 2b, where the case of LoS, the Euclidean distance dk is given by:

$$\mathrm{dk}=\sqrt{(L^2+{r_k}^2)} \quad (8)$$

$$\cos(\varphi\mathrm{k})=\cos(\psi\mathrm{k})=\frac{L}{d_k} \quad (9)$$

Substituting (8) and (9) in (6), the DC gain for the LoS components can be expressed as:

$$\mathrm{hk}=\frac{\mathcal{C}(m+1)L^{m+1}}{dk^{\frac{m+3}{2}}} \quad (10)$$

where $\mathcal{C}=\frac{1}{2\pi}AR_p\mathrm{O}(\psi\mathrm{t})\mathrm{g}(\psi\mathrm{t})$ is a constant. From Eq.(10), we can see that the DC channel gain decreases as the radial distance of the user increases. The position of the patient is considered to be random in order to obtain the statistical model of the channel gain. The radical distance of the patient follows a uniform distribution inside the circular photocell with cumulative distribution function (CDF) given by Eq. (11).[23,29-33]

$$F_{\Gamma_{VLC}}\left(SINR_{k,n,v}^{VLC}\right)=\frac{-1}{{r^2}_e}\mathcal{C}(m+1)L^{m+1}\frac{2}{m+3}\left(\frac{SINR_{k,n,v}^{VLC}}{\overline{SINR}_{k,n,v}^{VLC}}\right)^{\frac{-1}{m+3}}+\left(1+\frac{L^2}{re^2}\right) \quad (11)$$

4. The proposed hybrid RF/VLC channel model

Hybrid networks are particularly attractive for sensitive environments such as hospitals, as the combined radio-optical network can be flexibly configured to adapt to particular operation scenarios and their associated requirements. Due to the fact that the system doesn't suffer from interference, the coexistence of radio and optical communications could reduce the outage probability. Network adaptation in future hospitals is the key to secure, private, and high-performance operations.[1,34] IEEE 802.15.7 describes the link adaptation process when receiving a dimming request from a given user. In such cases, data communication is kept at a lower rate instead of breaking the network link. Similarly, the network adaptation in a coexisting optical-radio network can be made by the network controller. In our proposed work, the SDN controller switches the optical to radio or vice versa by some predefined rules with the help of Pareto simulated annealing (PSA). Hard switching or handover is used to efficiently switch between RF and VLC channels. Choosing the optimal VLC channel among the presented channels is an NP-hard problem, and solving such problems is usually carried out using heuristic approaches. We have formulated our fitness function based on several performance metrics to be used by PSA to choose the optimal VLC link.

4.1 Formulation of the fitness function

In this section, we present the analytical expressions of outage and blocking probabilities, total delay, packet error rate (PER), throughput, and system fairness to be used as input parameters for the PSA algorithm in the proposed hybrid RF/VLC scheme.

4.1.1 Outage and blocking probabilities, f1

Outage probability is widely used in hybrid RF/VLC networks to characterize the network's reliability requirements. It is the probability of having the SINR of the communication band falls below the SINR threshold. In our proposed scheme, it is the probability that the SINR of the VLC channel and the SINR of the RF channel fall below a given threshold. The blocking probability is the probability when the SINR of the VLC channel drops to zero. Hence, the outage probability of the RF sub-channel n and VLC sub-channel n is defined as the probability that the received SINR at the receiver, denoted by ($SINR_{k,n}^{RF}$) and $SINR_{k,n,v}^{VLC}$, respectively, is below a target threshold, denoted by $SINR_{k,n}^{rf\_th}$ and $SINR_{k,n,v}^{vlc\_th}$, respectively. Then, the reliability requirement is achieved by upper bounding the total outage probability of the hybrid RF/VLC system, denoted by $P_{out}^{RF/VLC}$, to a maximum threshold, denoted by P_{max}^{th}, is given by Eq. (12).

$$P_{out}^{RF/VLC} \leq P_{max}^{th} \tag{12}$$

Since the outage probability of the RF link is given by $P(SINR_{k,n}^{RF} < SINR_{k,n}^{rf\_th})$ which is the cumulative distribution function, CDF of RF, denoted by $F_{SINR_{RF}}(SINR_{k,n}^{rf\_th})$ given by Eq. (13) as:[23,32]

$$F_{SINR_{RF}}\left(SINR_{k,n}^{rf_{th}}\right) = 1 - \frac{1}{\Gamma(m)} G_{1,2}^{2,0}\left[\left(\frac{m}{\overline{SINR}_{k,n}^{RF}}\right) SINR_{k,n}^{rf\_th}\Big|_{m,0}^{1}\right] \tag{13}$$

In VLC networks, the VLC technology consists of LoS links from multiple VLC access points or transmitters, and the VLC LoS channels support successful communication services, while the blocked channels cannot provide high data rate transmission services.[30] The SDN controller will run the PSA algorithm to optimally choose a VLC link satisfying the network constraints. Outage occurs in VLC channel of the vth AP if the probability of SINR of VLC sub-channel n falls below a threshold; *i.e.*, $P(SINR_{k,n,v}^{VLC} < SINR_{k,n,v}^{vlc\_th})$ which is the CDF of VLC link, denoted by $F_{SINR_{VLC}}(SINR_{k,n,v}^{vlc\_th})$, and is represented by the binomial series by Eq.(14):[23]

$$F_{SINR_{VLC}}^{max}\left(SINR_{k,n,v}^{vlc_{th}}\right) = \sum_{k=0}^{N}(-1)^k\binom{N}{k}\theta^{N-k}\,\mathcal{X}^k\left(\frac{SINR_{k,n,v}^{vlc\_th}}{\overline{SINR}_{k,n,v}^{VLC}}\right)^{\frac{-k}{m+3}} \tag{14}$$

where $\theta = (1+\frac{L^2}{re^2})$, and $\mathcal{X} = \frac{1}{re^2}(\mathcal{C}(m+1)L^{m+1})^{\frac{2}{m+3}}$

Finally, the outage probability $P_{out}^{RF/VLC}$ of the hybrid RF/VLC system is given by Eq. (15).

$$P_{out}^{RF/VLC} = P(SINR_{k,n}^{RF} < SINR_{k,n}^{rf\_th}) \times P\left(SINR_{k,n,v}^{VLC} < SINR_{k,n,v}^{vlc_{th}}\right) = F_{SINR_{RF}}\left(SINR_{k,n}^{rf_{th}}\right) \times F_{SINR_{VLC}}^{max}(SINR_{k,n,v}^{vlc\_th}) \tag{15}$$

The blocking probability of a hybrid RF/VLC system is the probability that the SINR of the VLC link falls to zero; *i.e.*, $P_{blocking}^{VLC} = P(SINR_{k,n,v}^{VLC} = 0)$. It was taken different values for blocking probability in the range of [0 - 0.3].

Finally, Eq. (16) represents the outage and blocking probabilities of the hybrid RF/VLC scheme.[23,32]

$$f1 = P_{out}^{RF/VLC} \cap P_{blocking}^{VLC} = P_{out}^{RF/VLC} \times P_{blocking}^{VLC} \tag{16}$$

4.1.2 Packet error rate, f2

The packet error rate (PER) is an important factor in evaluating the performance of a wireless communication system. In the proposed system, we have considered un-coded packet transmission with a cyclic redundancy check that has the ability to detect but not correct any error. Hence, when an error occurs, the packet is dropped. Before starting the PER, it

is important to explain the BER since the PER for a packet of length Nb, is derived from BER.

For typical medical sensors, the QoS is characterized by BER < 10^{-10}.[31] The average BER of the hybrid RF/VLC network consists of the BER of the network operating under RF channels and VLC channels. The average BER of the network operating under RF channels, denoted by P_b^{RF} in Eq.(17) as:[23]

$$P_b^{RF} = \frac{1}{2\Gamma(a)2\Gamma(m)} \mathcal{G}_{2,2}^{1,3}\left(\frac{m}{b\overline{SINR}_{k,n}^{RF}}\right)|_{m,0}^{1,1-a} \quad (17)$$

where m is the RF fading factor. The average BER of the network operating under N VLC APs, denoted by P_b^{VLC}, is calculated from the VLC sub-channel n having no blocking probability. Therefore, the P_b^{VLC} is given as in Eq. (18).[23]

$$P_b^{VLC} = \frac{N}{2\Gamma(a)(m+3)} \sum_{k=0}^{N-1}(-1)^k \binom{N-1}{k} \theta^{N-1-k} \mathcal{X}^{k+1} \left(\overline{\mathrm{SINR}}_{\mathrm{k,n,v}}^{\mathrm{VLC}}\right)^{\frac{k+1}{m+3}} \times [\Lambda(\lambda\max, \alpha) - \Lambda(\lambda\min, \alpha)] - (1 - \mathrm{P}_{\mathrm{blocking}}^{\mathrm{VLC}}) \quad (18)$$

where m is the Lambertian radiation pattern given by Eq. (5), a=0.5, b=1, $\alpha = \frac{-(k+1)}{m+3}$, $\Lambda(\lambda, \alpha) = \lambda\alpha\mathcal{G}_{2,3}^{2,1}\left[b\lambda\,|_{1,a,-\alpha}^{1-\alpha,1}\right]$

Therefore, the average BER of the proposed RF/VLC scheme, denoted by PbRF/VLC, is given by Eq. (19).

$$\frac{\mathrm{PbRF}}{\mathrm{VLC}} = \frac{\left(1-\mathrm{F}_{\gamma_{VLC}}^{max}\left(SINR_{k,n,v}^{vlc\_th}\right)\right)P_b^{VLC} + \mathrm{F}_{\gamma_{VLC}}^{max}\left(SINR_{k,n,v}^{vlc\_th}\right)\left(1-\mathrm{F}_{\gamma_{RF}}\left(SINR_{k,n}^{rf\_th}\right)\right)P_b^{RF}}{1-P_{out}^{RF/VLC}} \quad (19)$$

Hence, PbRF/VLC should be bounded by a threshold to satisfy QoS requirements and can be rewritten as in Eq. (20).[23]

$$f2 = PER^{RF/VLC} = 1 - (1 - P_b^{RF/VLC})^{N_b} \quad (20)$$

s.t. $P_b^{RF/VLC} \leq \mathrm{BERthr}$

4.1.3 Throughput, f3

The throughput of a communication system is defined as the rate of successfully transmitted packets over the communication channel with a certain bandwidth. Due to the multiple VLC APs deployment (N=4), if a patient locates itself at an overlapped area, as in Fig. 2, an inter-cell interference (ICI) from adjacent cells may be caused. A packet is considered to be successfully transmitted when all of its Nb bits are successfully received at the destination. The total throughput achieved on all sub-channels is the sum of the achieved data rates of all sensors by VLC APs and RF APs. Therefore, the overall throughput of the hybrid RF/VLC system is given by Eq.(21):[23]

$$f3 = C^{RF/VLC} = \sum_{p=1}^{P}(p_{vlc}\eta_p{}^{VLC} + p_{RF}\eta_p{}^{RF}) \quad (21)$$

$$\eta_p{}^{VLC} = \sum_{k=1}^{K}\sum_{v\in\mathbb{N}^{VLC}}\sum_{n\epsilon\eta VLC}\frac{B_n^{VLC}}{2} log_2(1 + SINR_{k,n,v}^{VLC}) \times (1\text{-}P_{blocking}^{VLC}) \quad (22)$$

$$\eta_p{}^{RF} = \sum_{k=1}^{K}\sum_{n\epsilon\eta RF} B_n^{RF}\, log_2(1 + SINR_{k,n}^{RF}) \quad (23)$$

where p_{vlc}, p_{RF} are the link coefficients that can be either 0 if inactive or 1 if active. $\eta_p{}^{VLC}, \eta_p{}^{RF}$ are the total throughput of the network operating under VLC channels and RF channels, given by Eq. (22) and Eq. (23), respectively. B_n^{VLC} and B_n^{RF} represent the n sub-channel bandwidth of the VLC channel and RF channel, respectively. The scaling factor 1/2 is due to the Hermitian symmetry.[33] If the kth sensor (k ϵ Ƙ) is assigned to VLC AP v ϵ ℕVLC on the n sub-channel (n ϵ nVLC), the received signal-to-interference plus noise ratio (SINR) of the sensor k is expressed by Eq. (24).[27] The SINR observed by the receiver in the RF band expressed by Eq. (25) and $C^{RF/VLC}$ is the throughput of the hybrid RF/VLC network.

$$SINR_{k,n,v}^{VLC} = \frac{P_{n,v}^{VLC} h_{k,n,v}^{VLC} \mathfrak{r}^2}{\mathfrak{r}^2 \sum_{v'\epsilon\mathbb{N}}(P_{n,v'}^{VLC} h_{k,n,v'}^{VLC}) + \mathfrak{s}^{VLC} B_n^{VLC}} \quad (24)$$

where $P_{n,v}^{VLC}$ is the allocated transmitting optical power on the n sub-channel of the v VLC AP, $P_{n,v'}^{VLC}$ is the allocated transmitting optical power on the n sub-channel of the neighboring v' VLC AP, $h_{k,n,v}^{VLC}$ is the n sub-channel gain from the v VLC AP to k sensor assuming LoS expressed in Eq.(10), $\mathfrak{r}$ is photo-diode responsivity, and $\mathfrak{s}^{VLC}$ is the power spectral density (PSD) of noise at the PD.

The signal to interference plus noise ratio of the RF band is expressed as:

$$SINR_{k,n}^{RF} = \frac{P_n^{RF} h_{k,n}^{RF}}{P_n^{RF} h_{k,n}^{RF} + \mathfrak{s}^{RF} B_n^{RF}} \quad (25)$$

where P_n^{RF} is the allocated transmission power on the n sub-channel of RF AP; h_{kn}^{RF} is the channel gain of n sub-channel to k sensor expressed by Eq. (1). $\mathfrak{s}^{RF}$ is the RF thermal noise with spectral density of -174 dBm/Hz.[34] B_n^{RF} is the sub-channel bandwidth given by BRF/NRF, with BRF being the bandwidth of the RF AP.

4.1.4 The worst-case latency, f4

The worst-case latency denoted by TD is the sum of the end-to-end delay between the controller and sensor node k; kϵƘ, the queuing delay, and the handover delay. The queuing delay is the average time spent on the packet in the kth buffer before being sent to controller C. The handover delay, dented by THO, is the time it takes to do the handover process. It is defined as the time difference between the time of detection when there is a need for handover and the time to optimally select the communication link. Hence, the ultimate goal is to restrict the total delay to a given threshold: $TD \leq T_{th}$ in Eq. (26) shows TD:

$$f4 = \mathrm{TD} = (\mathrm{T_{propagation}} + \mathrm{T_{transmission}} + \mathrm{T_{Queue}} + \mathrm{T_{HO}})$$
$$\text{s. t. } \mathrm{T_{transmission}} < 5ms, TD \leq T_{th}, THO \leq VHO_{th} \quad (26)$$

where total propagation time is given by Eq.(27):

$$\mathrm{T_{propagation}} = \sum_{k=1}^{K} \frac{distance(k,C)}{light_{speed}} \quad (27)$$

The total transmission time is given by Eq. (28):

$$\mathrm{T_{transmission}} = \mathrm{PvlcTvlc} + \mathrm{PRFTRF} \quad (28)$$

where Pvlc is 1 if the VLC channel is used for communication and zero otherwise. Same is applied for RF channel, the time taken to transmit Nb packet size over VLC channel and RF

channel is given by Eq. (29) and Eq. (30), respectively.

$$\text{Tvlc} = \frac{N_b}{{\eta_p}^{VLC}} \quad (29)$$

$$\text{TRF} = \frac{N_b}{{\eta_p}^{RF}} \quad (30)$$

where N_b is packet size, ${\eta_p}^{VLC}$ is the data rate of VLC channel expressed in Eq. (22); ${\eta_p}^{RF}$ is the data rate of RF link expressed in Eq. (23); T_{HO} is the handover delay. The queuing delay is given by Eq.(31).

$$T_{queue} = \frac{1}{\mu - \lambda} \quad (31)$$

where μ is the service rate, and λ is the arrival rate. The controller's buffer is assumed to be modeled as M/M/1.[35]

4.1.5 System fairness, f5

We have adopted Jain's fairness index in order to measure the whole system's fairness.[36] The system is said to be fair when all the nodes are utilizing the network resources equally. Eq. (32) shows the system fairness, denoted by Fsys, where N_i is the number of nodes connected to access point i, excluding the priority-given nodes, since it is inefficient to calculate the system fairness when priority-given nodes and normal nodes are present. N_{AP} is the total number of access points (RF AP and VLC APs), $R_{j,i}$ is the data rate achieved at node j of access point i. Since we have three patients, each equipped with 12 nodes. Ni is the total number of nodes connected to access point i, j ϵ {1,…,36}.

$$f5 = \text{FSys} = \frac{\left(\sum_{i=1}^{N_{AP}} \sum_{j=1}^{Ni} R_{j,i}\right)^2}{N_{AP} \sum_{i=1}^{N_{AP}} \sum_{j=1}^{Ni} {R_{j,i}}^2} \quad (32)$$

4.2 Pareto Simulated Annealing (PSA)

Multi-objective optimization, also called multi-attribute optimization, solves problems that consist of more than one objective function to be simultaneously optimized. Many techniques have been addressed in the literature to deal with multi-objective optimization that can be classified into three approaches: a priori, a posteriori, and progressive.[25] The prior approach transforms the multi-objective function into a mono-objective one. Many methods are involved in the transformation issue, namely, goal programming, scalarization, and lexicographical, which typically return the Pareto optimal solution. The metaheuristic algorithm on a certain aggregation of the objective function at each run is referred to as multiruns-techniques that are inspired by the priori multi-objective approach. At each run, it is expected to reach a near-optimal solution to the problem that satisfies a certain preference structure. Even though it is quite a simple concept of multiruns-based techniques, determining effective and pertinent preference structures for multi-objective issues ahead of time is not easy.[25] As stated in section 4.1, the sub-objectives of the fitness function are explained and formulated. Hence, the final fitness function, denoted by F, is given by Eq. (33).

$$\text{F}=\max(w_1(1/f_1)+ w_2(1/f_2)+w_3(f_3)+ w_4(1/f_4) + w_5(f_5)) \quad (33)$$

s.t. $f_1 \leq P_{max}^{th}$, $f_2 \leq$ BERth, $f_4 \leq$Tth

We have applied the PSA to solve the optimization problem.[25] The multi-objective simulated annealing discusses different probabilistic acceptance rules aiming at increasing the probability of accepting nondominated solutions. Non-dominated solutions are solutions that have not dominated any generated solution so far. A Pareto Simulated Annealing (PSA) procedure was proposed first and based on a weak acceptance criterion.[37] In other words, any solution that does not dominate the current solution could be accepted with a certain probability. Since the computational complexity of the PSA is high, to decrease its effect on system performance, we assumed that the control messages between the sensors and the controller are sent out-of-band (*i.e.*, on dedicated paths). Inspired by the genetic algorithm (GA), a population-based metaheuristic, PSA considers a set of generated solutions (sample) to be improved at each temperature.[38] Each solution from the sample is improved if the newly accepted solution is at a distance from the closest solution to the former solution. This approach is performed by either increasing or decreasing the weights of objectives according to which the closest solution is better than the current solution. The new weights combination will be used for the evaluation step in the next iteration as well as for the probabilistic acceptance. PSA attempts to maintain uniformity while improving the sample of generated solutions. The probability of acceptance is given by Eq. (34).[25] Table 3 illustrates the PSA procedure.

$$\text{P(Accept Sc)} = \alpha \prod_{i=1}^{m} \min\left(1; \exp\left(\frac{\omega_i \Delta_{fi}}{T}\right)\right) + (1 - \alpha)\min\left(1; \max_{i=1,\ldots,m}\left(exp\left(\frac{\omega_i \Delta_{fi}}{T}\right)\right)\right) \quad (34)$$

where m stands for a number of objective functions denoted by fi assigned to m scalar-valued weights ω_i, i = 1, . . . , m, and a candidate solution Sc. A detailed explanation of PSA can be found.[39,40]

4.3 The proposed vertical handover scheme

The proposed vertical handover (VHO) scheme shown in Fig. 3 consists of a channel selection algorithm that allows the controller to choose the optimal channel for communication based on the channel condition and ensure the WBAN's QoS is achieved. Maintaining the WBAN's QoS is done by processing the request from the priority-given sensors without causing any delays that might affect the overall system performance. Therefore, once the controller receives a request for selecting a channel for communication from any sensor, it does the following steps:

Step 1: Check if this sensor is the priority-given sensor. If yes, then it checks if its priority buffer is empty or not. If the buffer is empty, then, it immediately serves this new priority request by running the vertical handover algorithm.

Step 2: Checks whether there is a standing request in its non-priority buffer. If so, it selects the request based on FIFO and runs the handover algorithm. If the non-priority buffer is

Table 3. Pareto simulating annealing algorithm.[25]

Input: A cooling schedule t; a starting temperature T↔T0; a starting sample of generated solutions ℑ; and initial memory ɱ↔ ℑ Output: The archive ɱ representing an approximation of the Pareto solutions set	
1:	repeat
2:	for each Sc ∈ ℑ do
3:	repeat
4:	Construct a neighboring solution Snew
5:	If Snew is not dominated by Sc then
6:	Update ɱ with Snew
7:	Select Scl (if exists) the closest solution to Sc
8:	Update weights of objectives in accordance with Sc and Snew partial dominance
9:	else
10:	Accept Snew with certain probability
11:	end if
12:	until Equilibrium condition
13:	end for
14:	Decrease temperature T
15:	until Cooling condition
16:	return ɱ

empty, it ends up.

Step 3: If the request coming to the controller is not a priority and the controller is not busy, then it runs the handover algorithm and ends up

Step 4: if the controller is busy, then it stores the request in its non-priority buffer and once the controller is not busy, it executes step 2.

After processing the request from a priority-given sensor, the controller executes the Pareto simulated annealing algorithm to optimally select the communication band. The following steps describe the link selection for communication.

Step 5: At the beginning of the simulation, an RF band is used for communication.

Step 6: While the communication band is RF, the controller monitors the VLC links and determines the best signal to interference plus noise ratio (SINR) link.

Step 7: Consequently, the controller checks if the best SINR of the VLC link is above the threshold. It executes the PSA algorithm. The PSA algorithm selects the VLC link, denoted by $SINR_{select}^{VLC}$, satisfying the system constraints. To avoid unnecessary handover or the ping pong effect, the controller checks if the SINR of the selected VLC link is greater than the threshold, then it does hard vertical handover, *i.e.*, it switches the communication channel from RF link to VLC link and calculates the handover delay.

Step 8: If the best SINR of VLC is equal to zero, then the blocking occurs, and the controller goes to step 5.

Step 9: If $SINR_{select}^{VLC}$ is not above a threshold and current time is less than vertical handover time threshold, then the controller executes step 6. That is the controller monitors the VLC links and determines the best SINR. However, if the current time is greater or equal to the handover time threshold, then the controller checks the SINR of the RF band. If SINR of RF band is greater or equal to SINR threshold (*i.e.* SINRRF $\geq SINR^{rf\_th}$), then the controller does handover from VLC link to RF link and calculates handover delay. However, if both the SINR of RF and VLC links are below the specified threshold, then an outage occurs.

5. Performance evaluation

We have evaluated the proposed hybrid RF/VLC system using MATLAB. We have run our scheme 50 times for each blocking probability and took the average to achieve 95% confidence interval. We have analyzed the communication quality, represented by the outage probability, with respect to different room height values. In addition, we have recorded the number of handovers under different blocking probabilities and different values for the vertical handover threshold. Moreover, we have recorded the delay for different scenarios and compared the delay when the system is VLC-based with RF/VLC based for both priority and non-priority conditions. Finally, we have compared the proposed RF/VLC network performance with Bao *et al.*[38] for the restless scenario and Gupta *et al.*[23] Simulation parameters are given in Table 4.

Table 4. Simulation parameters.

Parameters	Values
Room size	5m × 5m × 3m
Effective aperture of PD (A)	1(cm)^2
Semiangle at half power (ϕ1/2)	600
Field of view (ψ1/2)	600
Data rate of VLC link	1Gbps
Data rate of RF link	200 Mbps
Data rate threshold	3 Mbps
Optical filter gain (O(ψt))	1
Threshold delay Tth	110ms
Refractive index (n)	1.5
Optical to electrical conversion efficiency	0.64 A/W
Noise power spectral density	10−21 A2/Hz
BER threshold (BERthr)	10-10
LED wavelength	880nm
PD responsivity γ	0.53 A/W
RF transmitting power P_t^{RF}	200 mW
VLC transmitting power P_t^{VLC}	200mW
$SINR_{k,n,v}^{vlc\_th}$	15 dB
$SINR_{k,n}^{rf\_th}$	15 dB
Blocking probability, Pblocking	[0,0.05-0.3]
Number of RF sub-channels	32
Number of VLC sub-channels	16
Carrier frequency fRF	2.4 GHz
Carrier frequency fVLC	5 GHz

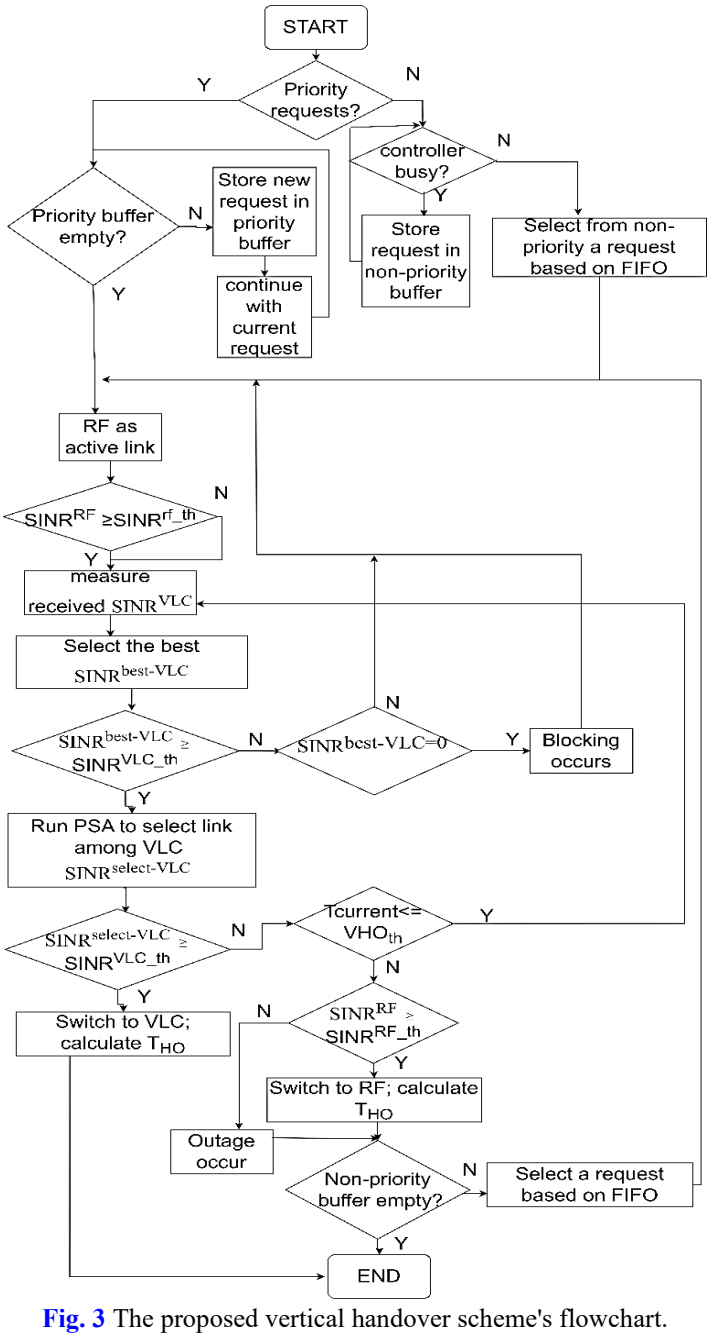

Fig. 3 The proposed vertical handover scheme's flowchart.

5.1 Network communication quality analysis

The communication quality of the network can be implicitly expressed by the reciprocal of the outage probability. Fig. 4 shows the variation of the outage probability with respect to the height of installation of the VLC LEDs, L. The outage probability increases (*i.e.* communication quality decreases) as the height of the room increases. This is because the signal power of VLC decreases with L, which is quite intuitive as the channel gain is monotonic decreasing function with respect to the distance between VLC transmitter and receiver. It is clear from the figure that the communication quality sharply decreases as the height of the room increases from 3.5 m to 3.8 m and keeps decreasing afterward.

5.2 Vertical handover analysis

We have focused on the average number of vertical handovers to evaluate the system performance under different values of handover thresholds such as 50, 60, 70, and 80 micro-seconds and different values of blocking probability for each simulation. The number of handovers has a negative impact on the overall system performance. Therefore, a fewer number of handovers operations is preferable. As shown in Fig. 5, a maximum number of vertical handovers is obtained with the least blocking probability under the least handover threshold since the system is operated under the RF communication band at the beginning and tries to run over VLC bands once the SINR of the VLC band is above a threshold. However, when blocking probability increases, the system will keep operating under RF band as long as no band of the VLC APs faces any blockage and whose SINR is above a threshold is

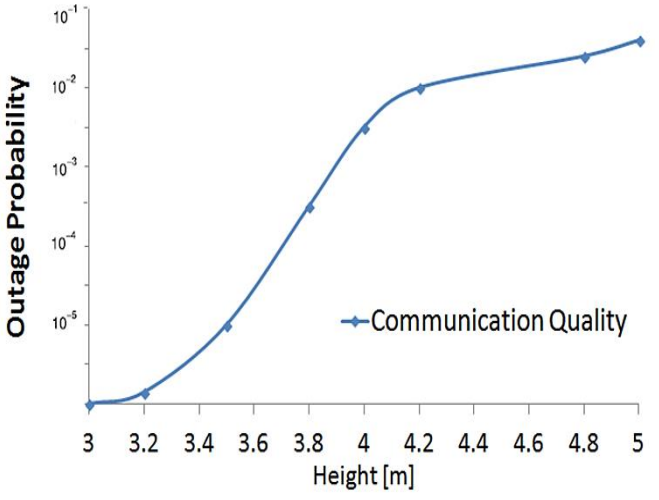

Fig. 4 Outage probability versus height of room.

detected. The number of vertical handovers drops by 60% as the threshold increases from 50 μs to 60 μs when the blocking probability is 0. Consequently, as the threshold value increases from 60 μs to 80 μs, the number of handover operations decreases by 20%. This interprets that an increase beyond the value of handover time threshold, which is 60 μs seconds as shown in Fig. 5, has slight effect on the number of handovers since the duration of handover surpasses the triggering threshold. In regard to blocking probability, it is obvious that when the blocking probability values are 0.05, 0.1, 0.15, 0.2, 0.25, and 0.3, the number of vertical handovers drops by 5%, 7%, 8%, 10%, 15%, and 20%, respectively, compared with the case of having no blocking probability in the system.

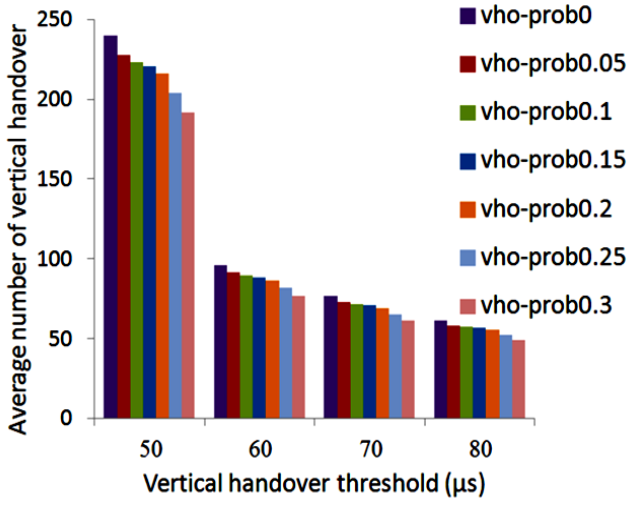

Fig. 5 Average number of VHO versus handover threshold.

5.3 Delay analysis

We have evaluated the proposed hybrid RF/VLC scheme in terms of delay under different values of blocking probabilities. Delay is a critical performance metric that reflects reliability, especially for priority-given sensors. It is necessary to point out that when the blocking likelihood increases, the system is most likely operating under the RF band. Hence, the system delay is more significant than when the system is operating under the VLC band. As we can see from Fig. 6, when the blocking probability doesn't exist in the system, the delay for the standalone VLC system is slightly less than that of the proposed system. However, when the blocking probability increases, the delay for the standalone system gradually increases, which is more than that of the proposed system. In both scenarios, the delay is less for priority-given sensors than for the rest of the sensor nodes. The proposed hybrid RF/VLC scheme achieves the QoS for WBANs. The average percentage of improvement of the proposed hybrid RF/VLC scheme for the priority scenario is 20% better than that for the non-priority scenario. In comparison between the proposed hybrid RF/VLC scheme and the standalone VLC scheme for priority scenarios, the average percentage of improvement of the proposed scheme is approximately 19% better than that of the VLC standalone scheme. Also, for non-priority scenarios, the average percentage of improvement of the proposed scheme is approximately 7% better than that of the VLC standalone scheme.

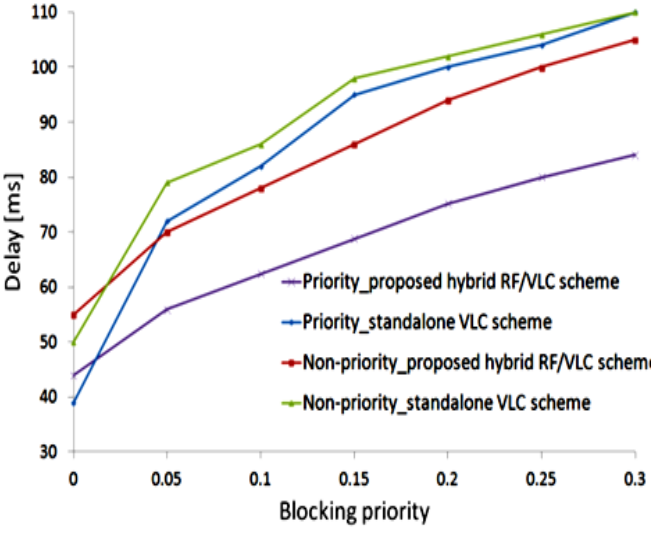

Fig. 6 Delay analysis.

5.4 Outage probability analysis

We have evaluated the outage probability of the proposed scheme under the maximum blocking probability of 0.3 for different values of signal to interference plus noise ratios in comparison with Bao *et al.*[38] and Gupta *et al.*[23] for the resting scenario. When blocking probability exists, fewer VLC links are available. Fig. 7 illustrates that as SINR increases, the outage probability decreases since the signal strength is strong, so switching from the RF band to the VLC band decreases the outage probability. In our scheme, the minimum number of handovers is obtained at maximum blocking probability since our scheme operates under the RF band at the beginning with a handover threshold time of 60 μs. However, in Gupta *et al.*[23] and Bao *et al.*[38] schemes, each system operates at the beginning under the VLC band, and a maximum number of handovers is obtained under maximum blocking probability. This explains the superiority of our proposed scheme over Bao

et al.[38] and Gupta *et al*.[23] schemes in terms of outage probability by 25% and 55%, respectively.

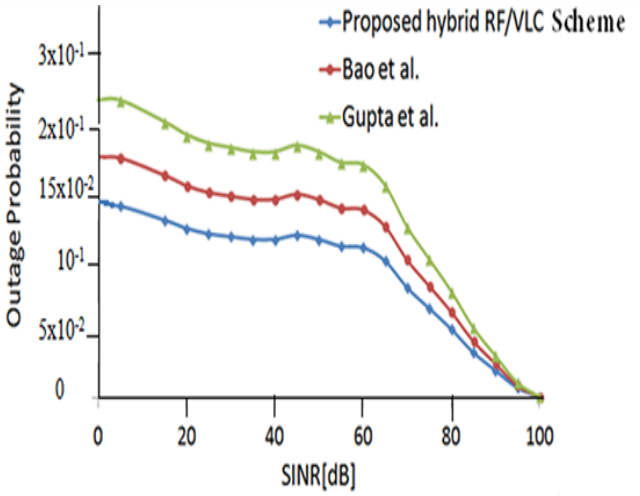

Fig. 7 Outage analysis.

5.5 Throughput analysis

In this section, we evaluated the performance of our proposed hybrid RF/VLC system based on the throughput in comparison with Bao *et al*.[38] and Gupta *et al*.[23] for the resting scenario. As seen in Fig. 8, the throughput is highly dependent on the blocking probability. As the blocking probability increases, the VLC LoS links can't provide high data rates, and consequently, the throughput decreases. In the work of Gupta *et al*.,[23] the system executes the hard switching without considering the threshold time for hard switching once the VLC SINR falls below a threshold. This causes a noticeable degradation in system performance. Bao *et al*.[38] formulated the threshold time for hard switching as probabilistic depending on the past durations of available and non-available VLC links. Therefore, as the blocking probability increases, the threshold time decreases, and the system is more likely to operate under the RF band. This explains the reason behind the superiority of our proposed system in terms of throughput over Bao *et al*.[38] and Gupta *et al*.[23] which is found to be approximately 40% and 60%, respectively, under different blocking probabilities.

5.6 Packet error rate (PER) analysis

Another important network performance metric is PER, which is given by Eq. (21). PER is affected by the signal to interference and noise ratio. As SINR increases, more signal strength is achieved; hence, VLC links are preferable to be used. Consequently, packets are transmitted with less error, and as a result, the packet error rate decreases under the VLC link transmission. However, when the blocking probability in VLC links occurs, then the choice of the RF links is preferable, which introduces packet errors during transmission due to interference, and as a result, the packet error rate increases. This is shown in Fig. 9. Once the VLC SINR falls below a threshold, the system executes the hard switching without considering the threshold time for hard switching.[23] This causes a noticeable degradation in system performance. The authors consider the threshold time for hard switching; however, the proposed threshold time is probabilistic and highly dependent on past events of available and non-available VLC links.[38] Therefore, as the blocking probability increases, the handover threshold decreases by a rate directly proportional to the past duration of VLC links availability. This only works well for moving patient scenarios to prevent unnecessary delays, and it doesn't work well for resting patient scenarios. So, the system is most likely operating under the RF band as the blocking probability increases. This explains the reason behind the superiority of our proposed system in terms of PER over Bao *et al*.[38] and Gupta *et al*.,[23] which is found to be approximately 39% and 50%, respectively.

5.7 System fairness analysis

The system fairness metric indicates the level of equality in utilizing the system resources among all sensor nodes. We recorded the system fairness under different blocking probabilities and compared the values with Bao *et al*.[38] and Gupta *et al*.[23] As shown in Fig. 10, it is obvious that when the blocking probability increases, a lesser number of VLC APs is available, and hence, lesser data rates are achieved at the sensor nodes. When the blocking probability is zero, all VLC links provide much higher data rates than RF links. Since each system of Bao *et al*.[38] and Gupta *et al*.[23] is operating at the VLC link, and our proposed system is operating at the RF link at the beginning; this causes a slightly better system fairness than Bao *et al*.[38] and Gupta *et al*.[23] than our proposed system when the blocking probability is zero. However, when the blocking probability increases, the controller at each patient will run the PSA algorithm to optimally select the link for transmission, whereas, in the work of Bao *et al*. and Gupta *et al*., each node runs the link selection algorithm to determine the suitable link for transmission. This causes rapid energy depletion, and as a result, fairness is not well achieved. Also, as blocking probability increases, unnecessary hard switching is observed by Bao *et al*.[38] and Gupta *et al*.[23] Since the hard switching threshold time is highly dependent on past events,[23,38] the hard switching threshold time is ignored, unnecessary handover is observed, causing the system to inefficiently allocate the system resources to sensor nodes, and as a result, the system fairness is not well achieved. The proposed hybrid RF/VLC scheme outperforms Bao *et al* [38] and Gupta *et al*.[23] schemes in terms of system fairness by approximately 8% and 10%, respectively.

5.8 Average percentage of improvement

The proposed RF/VLC scheme outperforms Bao *et al*.[38] and Gupta *et al*.[23] schemes in terms of different network performance metrics. Table 5 illustrates the average percentage of improvement (API) under different blocking probabilities of our proposed hybrid scheme over Bao *et al*.[38] and Gupta *et al*.[23] schemes.

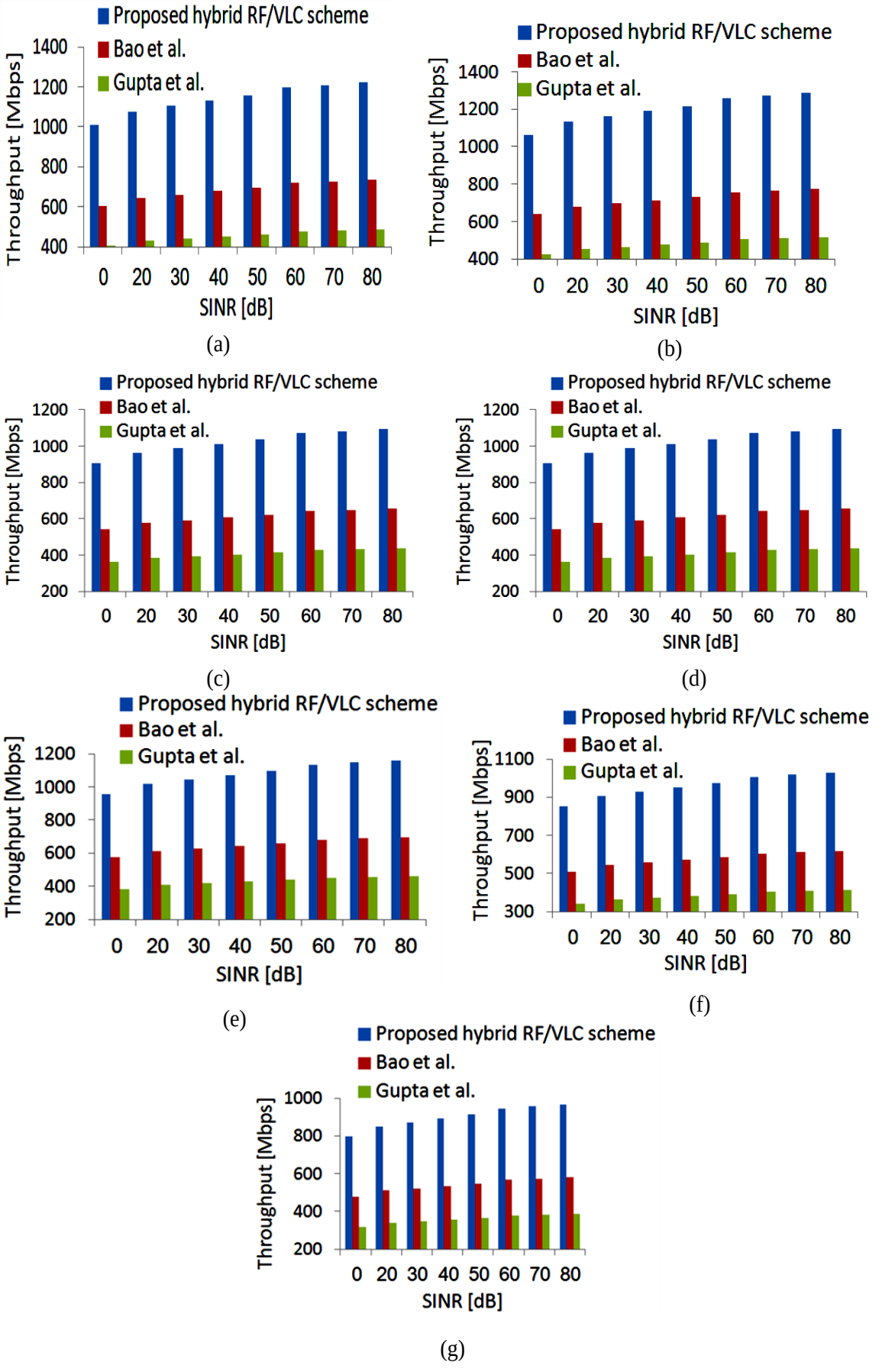

Fig. 8 Throughput analysis. (a) blocking probability 0, (b) blocking probability 0.05, (c) blocking probability 0.1, (d) blocking probability 0.15, (e) blocking probability 0.2, (f) blocking probability 0.25, (g) blocking probability 0.3.

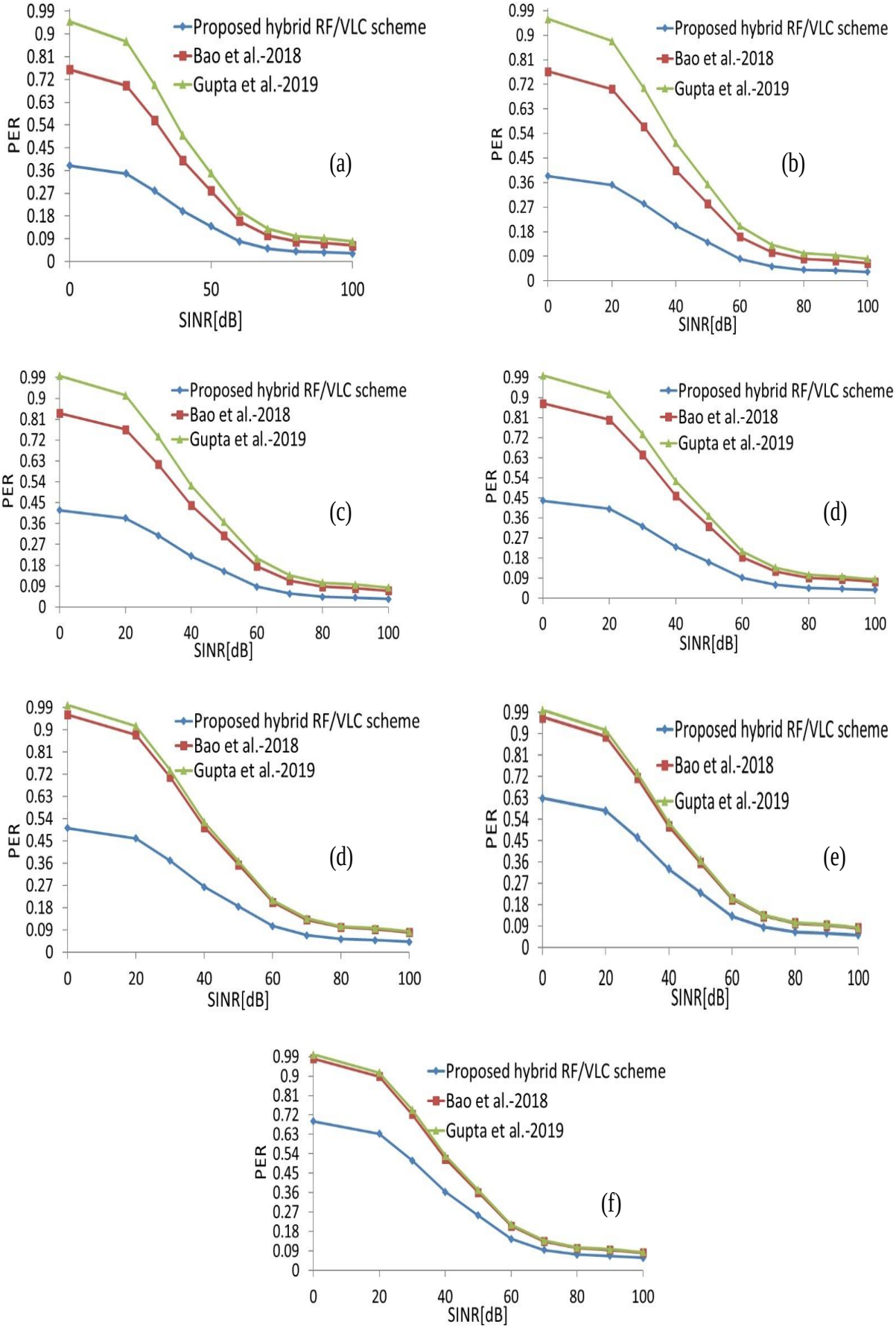

Fig. 9 Packet error rate analysis. (a) blocking probability 0, (b) blocking probability 0.05, (c) blocking probability 0, (d) blocking probability 0.15, (e) blocking probability 0.2, (f) blocking probability 0.25, (g) blocking probability 0.3.

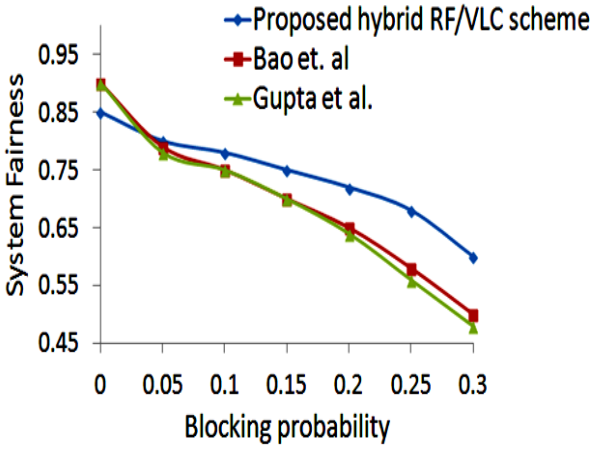

Fig. 10 System fairness analysis.

Table 5. API of the proposed hybrid RF/VLC scheme comparison.

Performance metric	Bao *et al.*[38]	Gupta *et al.*[23]
Outage probability	25%	55%
Throughput	40%	60%
PER	39%	50%
System fairness	8%	10%

6. Conclusion

In this article, we propose a vertical handover scheme for WBANs. Our objective is to avoid unnecessary handovers by taking into consideration a specific handover threshold time to optimize system performance. To specify this critical handover threshold, we have done simulations for the average number of handovers under different handover thresholds, which was noticeably dropped at 60 μs handover time; therefore, we set the threshold time for handover to 60 μs. In the work of Bao *et al*., the authors have formulated the hard switching threshold time as probabilistic depending on the past duration time of VLC availability and non-availability. This doesn't work well for resting scenarios, as in our present study, since it causes unnecessary handover. The proposed scheme concurrently considers the outage probability of the RF band and VLC band and the handover threshold time for selecting the communication band. Indeed, considering the handover threshold time has a positive impact on the overall network performance. Our proposed scheme gives high priority to sending emergency data and maximizes the system's fairness. Hence, the QoS is achieved. Our proposed hybrid RF/VLC system outperforms the standalone VLC system for system delay metric by approximately 19% for priority-based scenarios and by approximately 7% for non-priority-based scenarios. In addition, our proposed scheme operates under the RF band at the beginning of the simulation, which leads to a decrease in the number of handovers in the presence of blocking probability. Operating the system under an RF link at the beginning of the simulation results in better network performance than when operating under the VLC band as in benchmarked schemes (Bao's scheme and Gupta's scheme) in outage probability (approximately 25% to 55%), throughput (40% to 60%), packet error rate (39% to 50%), and system fairness (8% to 10%), respectively, when different blocking probabilities exist in the system. However, in the proposed scheme, we didn't consider the single point of failure, which will be considered in future work. Also, as a future work, the patient's mobility could be integrated into the proposed hybrid system. While the work offers significant contributions, there are critical limitations related to integration challenges, as integrating outage and blocking probabilities into the link selection algorithm, as well as implementing the proposed hybrid RF/VLC intra-SDWBAN architecture, may encounter compatibility issues with existing systems or infrastructure, leading to delays or complications in deployment. The challenges are to be considered as future work.

Conflict of Interest

There is no conflict of interest.

Supporting Information

Not applicable.

References

[1] I. Ahmed, T. Kumpuniemi, M. Katz, A hybrid optical-radio wireless network concept for the hospital of the future, *13th EAI International Conference on Body Area Networks*, 2020, 157-170, doi: 10.1007/978-3-030-29897-5_13.

[2] A. Ashimbayeva, N. Kalikulov, R. C. Kizilirmak, Hard and soft switching for indoor hybrid VLC/RF systems, 2017 IEEE 11th International Conference on Application of Information and Communication Technologies (AICT), September 20-22, 2017, Moscow, Russia, IEEE, 2017.

[3] H. Abuella, M. Elamassie, M. Uysal, Z. Xu, E. Serpedin, K. A. Qaraqe, S. Ekin, Hybrid RF/VLC systems: A comprehensive survey on network topologies, performance analyses, applications, and future directions, *IEEE Access*, 2021, **9**, 160402-160436, doi: 10.1109/ACCESS.2021.3129154.

[4] T. Komine, M. Nakagawa, Fundamental analysis for visible-light communication system using LED lights, *IEEE Transactions on Consumer Electronics*, 2004, **50**, 100-107, doi: 10.1109/TCE.2004.1277847.

[5] D. L. Hutt, K. J. Snell, P. A. Bélanger, Alexander graham Bell's PHOTOPHONE, *Optics and Photonics News*, 1993, **4**, 20, doi: 10.1364/opn.4.6.000020.

[6] D. K. Jackson, T. K. Buffaloe, S. B. Leeb, Fiat lux: a fluorescent lamp digital transceiver, *IEEE Transactions on Industry Applications*, 1998, **34**, 625-630, doi: 10.1109/28.673734.

[7] G. Pang, T. Kwan, C. H. Chan, H. Liu, LED traffic light as a

communications device, Proceedings 199 IEEE/IEEJ/JSAI International Conference on Intelligent Transportation Systems, October 5-8, 1999, Tokyo, Japan, IEEE, 1999.
[8] Y. Tanaka, S. Haruyama, M. Nakagawa, Wireless optical transmissions with white colored LED for wireless home links, 11th IEEE International Symposium on Personal Indoor and Mobile Radio Communications, PIMRC 2000, September 18-21, 2000, London, UK, IEEE, 2000.
[9] S. Aboagye, T. M. N. Ngatched, O. A. Dobre, H. V. Poor, Energy-efficient resource allocation for aggregated RF/VLC systems, *IEEE Transactions on Wireless Communications*, 2023, **22**, 6624-6640, doi: 10.1109/TWC.2023.3244871.
[10] F. Wang, F. Yang, C. Pan, J. Song, Z. Han, Hybrid VLC-RF systems with multi-users for achievable rate and energy efficiency maximization, *IEEE Transactions on Wireless Communications*, 2023, **22**, 6157-6170, doi: 10.1109/TWC.2023.3239840.
[11] A. Sathishkumar, S. Majji, T. Radhika Patnala, S. Rao Karanam, A. Kumar, M. Malyadri, Experimentation methodology of orthogonal frequency division multiplexing signals process using radio over fiber (RoF) system, 2022 International Virtual Conference on Power Engineering Computing and Control: Developments in Electric Vehicles and Energy Sector for Sustainable Future (PECCON), May 5-6, 2022, Chennai, India. IEEE, 2022.
[12] K. G. Rallis, V. K. Papanikolaou, P. D. Diamantoulakis, S. A. Tegos, A. A. Dowhuszko, M. A. Khalighi, G. K. Karagiannidis, Energy efficient cooperative communications in aggregated VLC/RF networks with NOMA, *IEEE Transactions on Communications*, 2023, **71**, 5408-5419, doi: 10.1109/tcomm.2023.3292486.
[13] D. A. Basnayaka, H. Haas, Design and analysis of a hybrid radio frequency and visible light communication system, *IEEE Transactions on Communications*, 2017, **65**, 4334-4347, doi: 10.1109/TCOMM.2017.2702177.
[14] Y. Wang, H. Haas, Dynamic load balancing with handover in hybrid Li-fi and Wi-Fi networks, *Journal of Lightwave Technology*, 2015, **33**, 4671-4682, doi: 10.1109/JLT.2015.2480969.
[15] F. Wang, Z. Wang, C. Qian, L. Dai, Z. Yang, Efficient vertical handover scheme for heterogeneous VLC-RF systems, *Journal of Optical Communications and Networking*, 2015, **7**, 1172-1180, doi: 10.1364/JOCN.7.001172.
[16] S. Liang, Y. Zhang, B. Fan, H. Tian, Multi-attribute vertical handover decision-making algorithm in a hybrid VLC-femto system, *IEEE Communications Letters*, 2017, **21**, 1521-1524, doi: 10.1109/LCOMM.2017.2654252.
[17] O. Haddad, M. A. Khalighi, S. Zvanovec, M. Adel, Channel characterization and modeling for optical wireless body-area networks, *IEEE Open Journal of the Communications Society*, 2020, **1**, 760-776, doi: 10.1109/OJCOMS.2020.2999104.
[18] C. Le Bas, S. Sahuguede, A. Julien-Vergonjanne, A. Behlouli, P. Combeau, L. Aveneau, Human body impact on mobile visible light communication link, 2016 10th International Symposium on Communication Systems, Networks and Digital Signal Processing (CSNDSP), July 20-22, 2016, Prague, Czech Republic, IEEE, 2016.
[19] U. F. Siddiqi, S. M. Sait, M. S. Demir, M. Uysal, Resource allocation for visible light communication systems using simulated annealing based on a problem-specific neighbor function, *IEEE Access*, 2019, **7**, 64077-64091, doi: 10.1109/ACCESS.2019.2917051.
[20] W. A. Cahyadi, T. I. Jeong, Y. H. Kim, Y. H. Chung, T. Adiono, Patient monitoring using Visible Light uplink data transmission, 2015 International Symposium on Intelligent Signal Processing and Communication Systems (ISPACS), November 9-12, 2015, Nusa Dua Bali, Indonesia. IEEE, 2015.
[21] D. R. Dhatchayeny, A. Sewaiwar, S. V. Tiwari, Y. H. Chung, EEG biomedical signal transmission using visible light communication, 2015 International Conference on Industrial Instrumentation and Control (ICIC), May 28-30, 2015, Pune, India, IEEE, 2015.
[22] W. Ding, F. Yang, H. Yang, J. Wang, X. Wang, X. Zhang, J. Song, A hybrid power line and visible light communication system for indoor hospital applications, *Computers in Industry*, 2015, **68**, 170-178, doi: 10.1016/j.compind.2015.01.006.
[23] A. Gupta, P. Garg, N. Sharma, Hard switching-based hybrid RF/VLC system and its performance evaluation, *Transactions on Emerging Telecommunications Technologies*, 2019, **30**, e3515, doi: 10.1002/ett.3515.
[24] K. Amine, Multiobjective simulated annealing: principles and algorithm variants, *Advances in Operations Research*, 2019, **2019**, 8134674, doi: 10.1155/2019/8134674.
[25] M. D. Yacoub, J. V. Bautista, L.G. de Rezende Guedes, On higher order statistics of the Nakagami-m distribution, *IEEE Transactions on Vehicular Technology*, 1999, **48**, 790-794, doi: 10.1109/25.764995.
[26] H. Yang, A. Alphones, W. D. Zhong, C. Chen, X. Xie, Learning-based energy-efficient resource management by heterogeneous RF/VLC for ultra-reliable low-latency industrial IoT networks, *IEEE Transactions on Industrial Informatics*, 2020, **16**, 5565-5576, doi: 10.1109/TII.2019.2933867.
[27] A. Prudnikov, Y. Brychkov and O. Marichev, Integrals and Series: More Special Functions, 1986.
[28] J. M. Kahn, J. R. Barry, Wireless infrared communications, *Proceedings of the IEEE*, 1997, **85**, 265-298, doi: 10.1109/5.554222.
[29] L. Yin, W. O. Popoola, X. Wu, H. Haas, Performance evaluation of non-orthogonal multiple access in visible light communication, *IEEE Transactions on Communications*, 2016, **64**, 5162-5175, doi: 10.1109/TCOMM.2016.2612195.
[30] H. Yang, A. Alphones, W.-D. Zhong, C. Chen, X. Xie, Learning-based energy-efficient resource management by heterogeneous RF/VLC for ultra-reliable low-latency industrial IoT networks, *IEEE Transactions on Industrial Informatics*, 2020, **16**, 5565-5576, doi: 10.1109/TII.2019.2933867.
[31] A. Julien-Vergonjanne, S. Sahuguède, L. Chevalier, Optical wireless body area networks for healthcare applications, *Optical Wireless Communications*, 2016, 569-587, doi: 10.1007/978-3-319-30201-0_26.

[32] S. I. Chu, SER and PER performance of packet decode-and-forward relaying with generalized order selection combining, *IEEE Wireless Communications Letters*, 2014, **3**, 449-452, doi: 10.1109/LWC.2014.2339278.
[33] H. Zhang, N. Liu, K. Long, J. Cheng, V. C. M. Leung, L. Hanzo, Energy efficient subchannel and power allocation for software-defined heterogeneous VLC and RF networks, *IEEE Journal on Selected Areas in Communications*, 2018, **36**, 658-670, doi: 10.1109/JSAC.2018.2815478.
[34] S. M. Ahsan Kazmi, N. H. Tran, W. Saad, Z. Han, T. M. Ho, T. Z. Oo, C. S. Hong, Mode selection and resource allocation in device-to-device communications: a matching game approach, *IEEE Transactions on Mobile Computing*, 2017, **16**, 3126-3141, doi: 10.1109/tmc.2017.2689768.
[35] K. Salah, A queueing model to achieve proper elasticity for cloud cluster jobs, 2013 IEEE Sixth International Conference on Cloud Computing, June 28 - July 3, 2013, Santa Clara, CA, USA. IEEE, 2013.
[36] R. Jain, A. Durresi and G. Babic, Throughput Fairness Index: An Explaination, 1984.
[37] P. Czyżżak, A. Jaszkiewicz, Pareto simulated annealing: a metaheuristic technique for multiple-objective combinatorial optimization, *Journal of Multi-Criteria Decision Analysis*, 1998, **7**, 34-47, doi: 10.1002/(sici)1099-1360(199801)7:134::aid-mcda161>3.0.co;2-6.
[38] X. Bao, A. A. Okine, W. Adjardjah, W. Zhang, J. Dai, Channel adaptive dwell timing for handover decision in VLC-WiFi heterogeneous networks, *EURASIP Journal on Wireless Communications and Networking*, 2018, **244**, 1-15, doi: 10.1186/s13638-018-1257-4.
[39] H. Tabassum, E. Hossain, Coverage and rate analysis for co-existing RF/VLC downlink cellular networks, *IEEE Transactions on Wireless Communications*, 2018, **17**, 2588-2601, doi: 10.1109/TWC.2018.2799204.
[40] Z. Becvar, M. Najla, P. Mach, Selection between radio frequency and visible light communication bands for D2D, 2018 IEEE 87th Vehicular Technology Conference, Porto, Portugal, IEEE, 2018.